The regulatory effect of purinergic P2X7Rs on the excitatory neurotransmission and the mouse model of schizophrenia

PhD thesis

Lumei Huang

Semmelweis University
Doctoral School of János Szentágothai

Supervisors: Beáta Sperlágh, MD, PhD, D.Sc
Official Reviewers of the PhD Dissertation:
Czirják Gábor, PhD, D.Sc; Judit Veres, PhD;
Head of the Complex Examination Committee:
László Köles, MD, PhD

Members of the Complex Examination Committee:
Dóra Zelena, PhD, D.Sc; György Lévay, PhD

Budapest

2024

1. Introduction

Purinergic signalling systems have received extensive research attention in both physiological and pathological conditions due to the discovery that “cellular energy currency” ATP could be released from cell into the extracellular space where it communicates with neighboring cells. As one of the most important receptors, ATP-gated ionotropic purinergic P2X7 receptor is particularly thought to be relevant to pathological conditions due to its low affinity to extracellular ATP. Although the protein and RNA expression of P2X7Rs in neurons have been documented, the neuronal expression of P2X7Rs and its contribution to neurotransmission are still controversial. The dentate gyrus (DG), the “gate” of classic trisynaptic circuit, serves as the important connection station between the entorhinal cortex (EC) and the rest of the hippocampus regions. However, it is unclear whether P2X7Rs express on DG and further participate in the regulation of excitatory neurotransmission. Moreover, the DG is subject to the development of schizophrenia (SCZ) in both patients and rodents. Although a few studies have reported that genetic ablation and pharmacological inhibition of P2X7Rs significantly alleviated phencyclidine (PCP)-induced schizophrenia symptoms, the role of P2X7Rs in PCP-induced

neurodevelopment model of SCZ and the involvement of DG in this process are still largely unknown.

Therefore, the aim of this work was to investigate the role of axonal terminal P2X7Rs in excitatory neurotransmission in mouse dentate gyrus granule cells (DG-GC) and its potential mechanisms. In addition, the present study was aimed at investigating whether genetically deleted P2X7Rs could alleviate postnatal PCP-induced SCZ-like symptoms in mice and how DG synapse (EC-GC) responds to this postnatal PCP treatment.

2. Objectives

ATP-gated P2X7Rs play a crucial role in brain diseases and neuroinflammation. Although the role of P2X7Rs in the regulation of neurotransmission has been repeatedly reported, whether neuronal P2X7Rs are directly involved in this process remains controversial. Meanwhile, the role of P2X7Rs in neurodevelopmental models of schizophrenia remains unclear. Therefore, this study was designed with a variety of approaches including whole-cell patch clamp, viral injection, Ca^{2+} imaging, immunohistochemistry and animal models to achieve the following objectives:

To investigate the role of P2X7R in excitatory neurotransmission onto mouse DG GCs and understand whether the regulatory effect shows a pathway specificity in DG

To address the potential effects of P2X7Rs on postnatal phencyclidine (PCP)-induced schizophrenia model in mice and explore the potential mechanism in EC-GC synapse

3. Methods

3.1 Animals

In our project, we used only C57Bl/6J mice. Both wild-type mice and P2rx7-/- mice were homebred. All animals were kept under a standard 12 h light/12 h dark cycle with food and water provided ad libitum.

3.2 Brain slices preparation and whole-cell patch-clamp recording

Mice were anesthetized by inhaling forane. Whole brains were cut in ice-cold cutting solution (in mM: 85 NaCl, 2.5 KCl, 2 $MgCl_2$, 0.5 $CaCl_2$, 1.25 NaH_2PO_4, 24 $NaHCO_3$, 25 glucose and 75 sucrose. Then the slices were incubated in ACSF composed of (in mM: 126 NaCl, 2.5 KCl, 2 $CaCl_2$, 2 $MgCl_2$, 1.25 NaH_2PO_4, 26 $NaHCO_3$ and 10 glucose) and bubbled with 95% O_2 + 5% CO_2 for 30 min at 34 °C. All recordings were performed at room temperature and were performed using whole-cell patch-clamp technique. Axopatch 1D amplifier and Digidata 1322A data acquisition system were used for recording. DG GCs were visualized by Olympus BX50WI Differential. Glass pipettes have a resistance of approximately 4-7 MΩ, pipettes greater than 7 MΩ and less than 4 MΩ were discarded.

3.3 Virus injection

To determine the participant of EC-GC pathway and its Ca^{2+} mechanism, we injected pAAV1-hSynapsin1-axon-GCaMP6s into EC (LEC: -3.8 mm anteroposterior (AP), ±3.9 mm mediolateral (ML) and -4.7 mm dorsal-ventral (DV); MEC: -4.72 mm (AP), ±3 mm (ML), -4 mm (DV)). The virus solution was diluted in the sterilized 0.1 mM PB buffer at a ratio of 1:10 for P2X7Rs immunostaining and Ca^{2+} imaging. The injection volume in different experiments was 60 nl in total for each side via the MicroSyringe Pump Controller system.

3.4 Immunostaining

After two weeks' expression, we did the P2X7Rs antibody immunostaining to identify the expression of P2X7Rs on the EC-GC axonal terminals. The post-fixed brains from both WT and P2rx7-/- injected with virus were sliced at 40 μm by using Leica vibratome. Slices were incubated in citrate buffer (pH 6) for 30 minutes at 85 °C after washing with PBS. Then, brain slices were blocked in PBS buffer consisting of 1% BSA, 5% FBS and 0.2% Triton X-100 for 1h at room temperature. We next incubated the slices with primary antibody. The primary antibody rabbit anti-P2X7Rs (1:100) and chicken anti-GFP (1:1000) were diluted in above blocking buffer for 2 nights at

4°C. The slices were washed with PBS. The biotinylated antibody containing 10% BSA, goat serum, and biotinylated anti-rabbit IgG were used to incubate the slices for 1h at room temperature. After PBS wash, the slices were incubated with the secondary antibodies 594-conjugated streptavidin (1:500) and 488-conjugated anti-chicken antibody (1:1000) for 1h at RT. Subsequently, sections were mounted on glass slides with ProLong Gold for C2 confocal imaging.

3.5 Ca^{2+} imaging

After two weeks' virus expression, mice were anesthetized by forane and hippocampal slices were prepared as described previously to detect the Ca^{2+} influx in EC boutons. We utilized an upright A1R MP+ multiphoton confocal microscope (NIKON) with a water immersion objective of NA 1.10, WD 2.0 (CFI75 Apochromat 25XC W 1300) and a 680-1040 nm titanium sapphire laser view and scan slices with axonal GCaMP reporter. We used a resonant scanner, at 30 Hz sampling rate, 920 nm wavelength, and 15 mW laser power to detect the Ca^{2+} related fluorescence. A monopolar stimulus isolator unit equipped with a sharp capillary placed either at the middle layer (MPP) or outer layer of molecular layer (LPP), was used to deliver the electric pulses. Scanning images were captured by

NIS software for further data analysis. The images were subsequently imported into the suite2p software for the imaging registration. To extract fluorescence traces and spikes in regions of interest (ROI) with the equation of: Fc= F-0.7*Fneu (Fc means corrected fluorescence value; F stands for the raw fluorescence intensity; Fneu means the neuropil-induced fluorescence intensity; 0.7 is the neuropil coefficient). We used python spyder script to subtract baseline fluorescence from peak fluorescence, subsequently obtained ΔF.

3.6 Animal model and behavior tests

We subcutaneously injected the PCP 10 mg/kg or an equal volume of saline into the male pups at P7, P9, and P11. At 3 weeks of age, the mice were weaned and separated into 3-5 mice per cage. We did locomotor activity test in open field, spontaneous alteration and novel object recognition tests in T-maze, the social preference in three chamber test, prepulse inhibition (PPI) test in acoustic startle box.

3.7 Statistics

The pClamp 10.2 was used to analysis electrophysiological recordings. GraphPad Prism 8.0.2 was used for statistical analyses. The Kolmogorov-Smirnov test was used for

cumulative probability. For two groups, the paired t-test and unpaired t-test were used. To compare multiple groups, one-way ANOVA (with or without repeated measures) and two-way ANOVA followed by the Dunnett-test and Tukey test were used. The data are presented as the means ± SEMs. Sample sizes were chosen based on the value sufficient to observe statistical significance in prior studies. Statistical significance was determined when $p^{*}<0.05$; $p^{**}<0.03$; $p^{***}<0.01$, ns: not significant.

4. Results

4.1 Activation of P2X7R modulated DG GC excitatory neurotransmission from presynaptic site

To understand whether the genetic ablation of P2X7Rs could change the excitatory neurotransmission onto DG GCs, we examined NMDA receptor-mediated excitatory postsynaptic currents in the presence (sEPSC) and absence (mEPSCs) of action potential propagation. To investigate the direct participant of P2X7Rs in this process, we applied to the P2X7Rs potent agonist BzATP and selective antagonist JNJ-47955567.

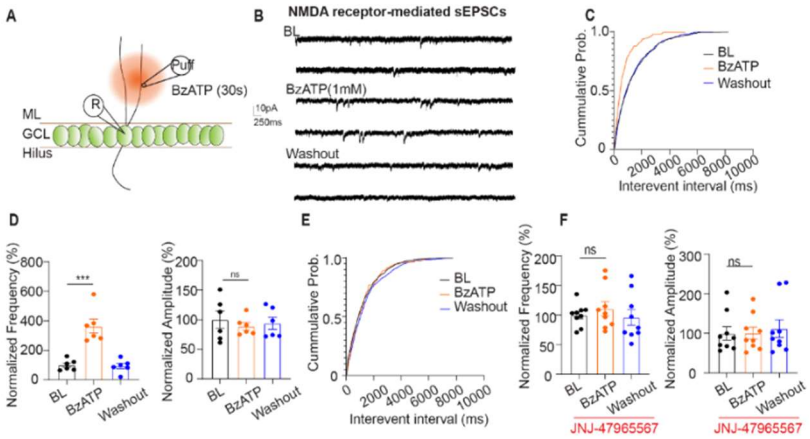

Figure 1. NMDA receptor-mediated DG GC sEPSC by pharmacological manipulation of P2X7Rs.

We directly applied BzATP (1 mM) via a fast drug application system (Figure 1A) to the molecular layer of DG for 30s after baseline recording, we found that the frequency of NMDA receptor-mediated sEPSC dramatically increased (Figure 1B-D). Remarkably, 1mM BzATP-induced potentiation was efficiently suppressed by bath application of P2X7R selective antagonist JNJ-47955567 (Figure 1E and F). We also recorded the NMDA receptor-mediated mEPSCs in the absence of action potential. Unsurprisingly, we also found that 1 mM BzATP increased the frequency of NMDA receptor-mediated mEPSCs and the increase was reversed by P2X7Rs antagonist JNJ-47965567 (Figure 2A and B). However, BzATP-induced effect showed a

concentration dependent manner, since 300 uM BzATP puff did not change the frequency (Figure 2C).

Altogether, above data suggested that P2X7Rs directly participate in the regulation of DG GC excitatory neurotransmission from the presynaptic sites.

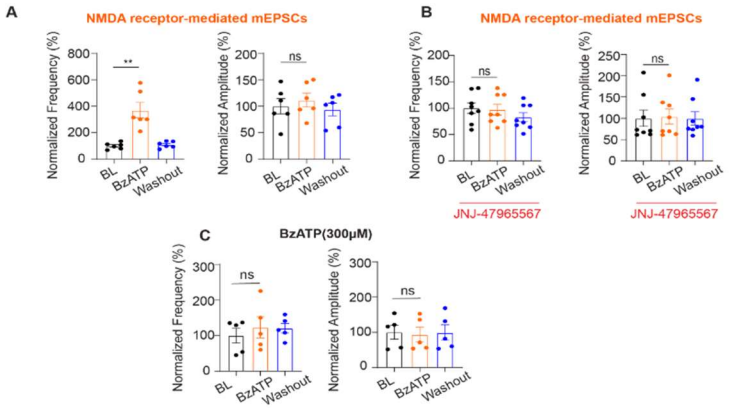

Figure 2. NMDA receptor-mediated mEPSC on DG GCs by pharmacological manipulation of P2X7Rs.

4.2 Regulation of DG-GC excitatory neurotransmission by P2X7Rs activation originates from the EC-GC pathway

Previous data has shown that acute activation of P2X7Rs lead to the increase of DG GCs glutamate release by changing the frequency, indicating the involvement of the presynaptic site, but it is still unclear whether this regulatory effect displays the

input specificity. In this project, we mainly stimulated EC-GC and MC-GC inputs. The stimulation-evoked excitatory postsynaptic currents (EPSC) and paired pulse ratio, which referred to presynaptic mechanism, have been recorded. In the LPP, we found that 1 mM BzATP application potentiated the 1st pulse-induced EPSC current amplitude, contributing to the decrease of PPR (Figure 3B-D). However, the P2X7Rs antagonists JNJ-47965567 (Figure 3E) and A438079 blockage inhibited the effect of BzATP (Figure 3C). Moreover, we had the similar observation when the MPP was targeted. (Figure 3G). Remarkably, when we placed the stimulating electrode into the inner molecular layer of DG where the MC-GC fibers present, we did not obtain the similar results with EC-GC fibers stimulation (Figure 4). Therefore, the regulatory effect of P2X7Rs activation on excitatory neurotransmission originated from the EC-GC pathway.

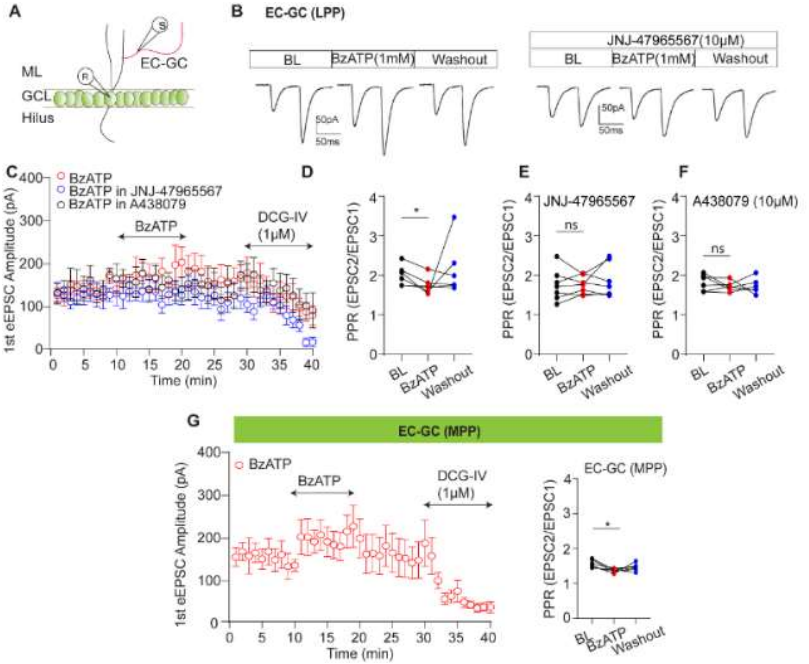

Figure 3. P2X7Rs regulate excitatory neurotransmission onto DG GCs originated from through the EC-GC pathway, including LPP and MPP.

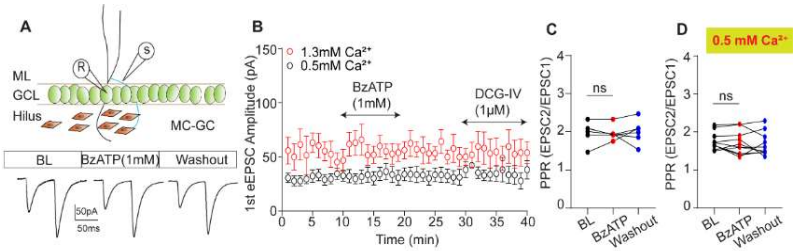

Figure 4. MC-GC pathway did not contribute to P2X7Rs activation-regulated DG-GC neurotransmission.

4.3 Activation of P2X7Rs on EC boutons directly promoted the Ca^{2+} influx

A line of evidence suggest that the activation of P2X7Rs caused Ca^{2+} influx via the channel itself, but no data has indicated whether P2X7Rs directly express on EC GC (perforant path) boutons to elicit the influx of Ca^{2+} into these boutons, followed by the increasing of neurotransmission. To clarify this, we applied to 1 mM BzATP to activate the P2X7Rs and scanned the fluorescence intensity change in the LPP. We found that 1mM BzATP application increased the peak of the fluorescence intensity in comparison with the baseline (Figure 5A and B). The BzATP-induced elevation was inhibited by pre-incubation of P2X7Rs antagonist JNJ47965567 (Figure 5C and D). Additionally, we observed the similar results when we targeted the MPP (Figure 5E and F).

Together, all these data suggested that the activation P2X7Rs on boutons by agonist directly increased the stimulation evoked Ca^{2+} influx in both LPP and MPP.

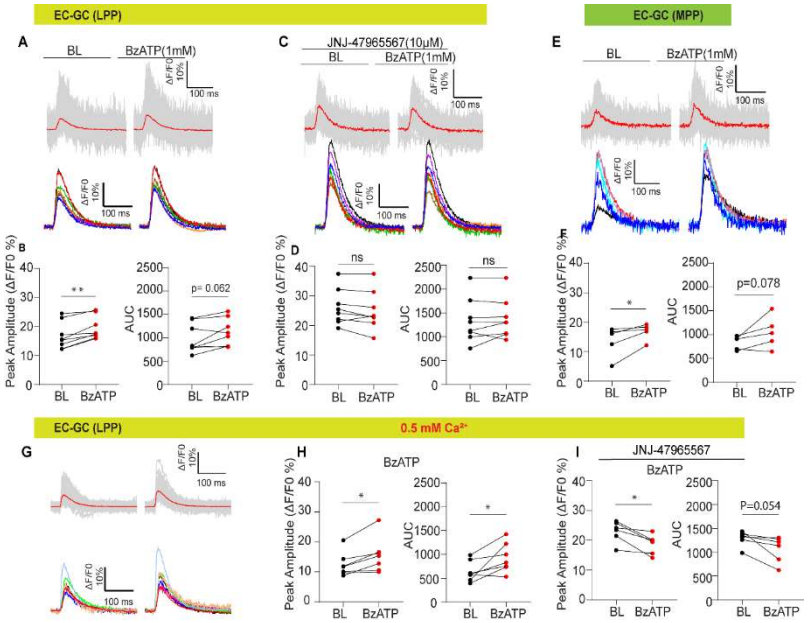

Figure 5. P2X7Rs activation induced-Ca^{2+} influx on LPP and MPP axonal boutons.

4.4 Genetic ablation of P2X7R attenuates postnatal PCP-induced schizophrenia-like symptoms in mice

To identify the role of P2X7Rs in pathological conditions, we mainly established PCP-induced schizophrenia model in mice by injecting PCP into male pups at P7, 9, 11 and checked EC GC synapse alteration and the behaviour alterations in both juveniles and adults.

We investigated whether genetic ablation of P2X7Rs changed synaptic plasticity induced by PCP treatment. We first measured the AMPA/NMDA ratio at EC GC synapses on P21-28 after postnatal PCP or saline treatment. We found AMPA/NMDA ratio robustly increased when animals were treated with PCP in WT, indicating postanal PCP treatment impaired the EC GC synapse by altering AMPA/NMDA ratio (Figure 6A and B). Importantly, AMPA/NMDA ratio kept unchanged in P2X7R deficient animals (Figure 6A and B). These data addressed that P2X7Rs deficiency resisted the alteration of synapse plasticity under pathological condition. We did not find the genotype difference in AMPA/NMDA ratio in both DG GCs and CA1 pyramidal cells, although AMPA and NMDA receptor components changed in pyramidal cells (Co-author paper 1).

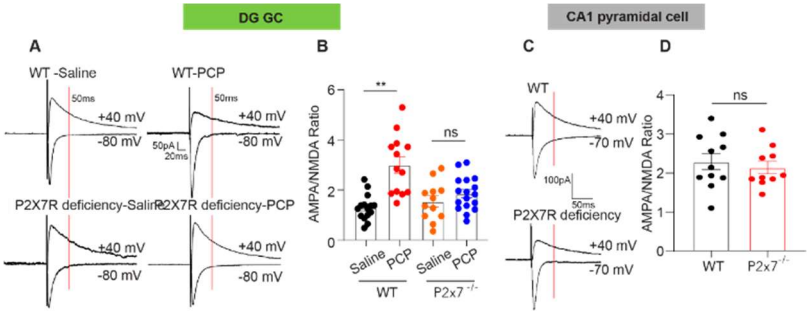

Figure 6. AMPA/NMDA ratio in DG GCs.

We next investigate the behaviour alteration in both juveniles and young adults. In both T-maze and open field diagram, PCP treated WT animals showed significantly longer moving distance in 10 minutes compared to saline treatment in both T-maze and open field diagram. However, PCP treatment-induced hyper locomotor activity was missing in P2X7R deficient mice (Figure 7A), suggesting that the genetic ablation of P2X7Rs alleviated PCP-induced positive symptoms. Additionally, PCP treatment decreased the ability to remember the previously travelled arms in T-Maze alteration test. However, P2X7Rs deficient animals did not show disturbance of spontaneous alterations after PCP treatment (Figure 7B). This suggested that the genetic absence of P2X7R also suppressed the PCP-induced working memory impairment.

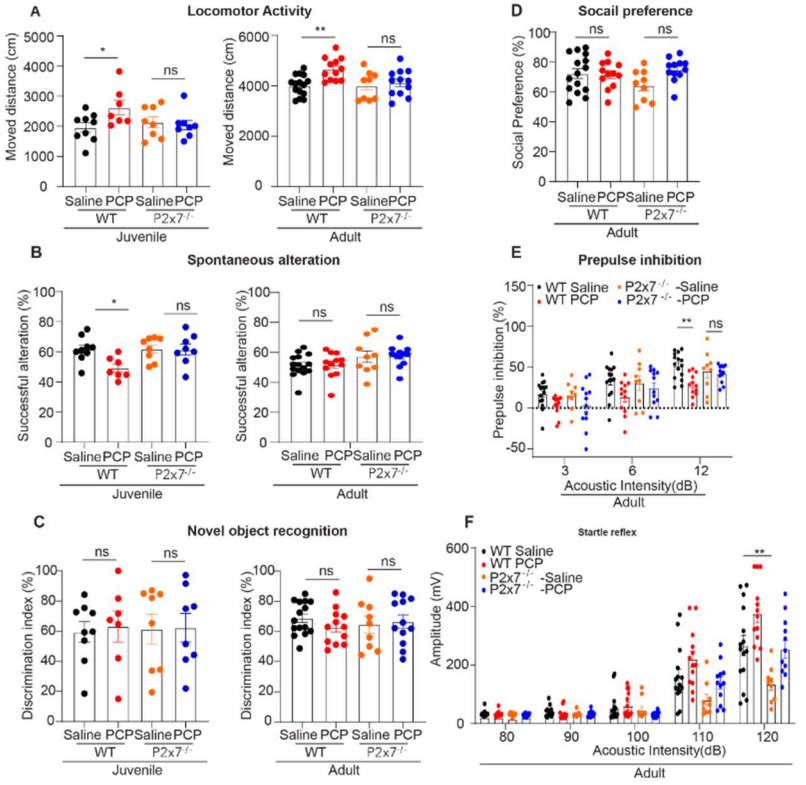

Figure 7. Behavioural testing of two genotypes at different ages.

In the acoustic startle reflex experiment, PCP treated animals showed an impairment of prepulse inhibition (PPI) only in WT but not in P2X7R deficient mice (Figure 7E), addressing that the absence of P2X7Rs also attenuated the PCP-induced alteration of sensory gating. Together, these data indicated that the genetic

ablation of P2X7Rs alleviated postnatal PCP induced schizophrenia-like symptoms in both juvenile and young adults.

To understand the role of P2X7Rs in another pathological condition, we established inflammatory pain model by injecting CFA into the left hind paw intra-plantar (Co-author paper 2). Compared to pre-CFA injection, CFA injection decreased the paw withdrawal latency (PWL) in all groups, suggesting CFA injection successfully led to thermal hypersensitivity. Remarkably, the injection of 300 nM P2X7Rs antagonist A438079 acutely relieved the pain as the time of PWL increased at 0 min (Figure 8).

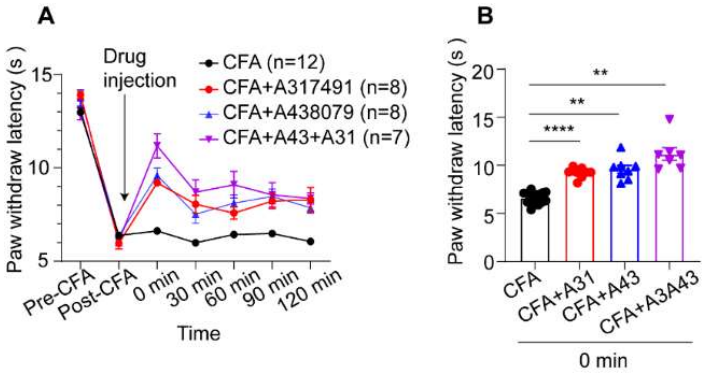

Figure 8. Paw withdrawal latency (PWL) in different groups.

5. Conclusions

The data presented in this thesis highlights the important role of presynaptic P2X7Rs in excitatory neurotransmission in postnatal PCP-induced schizophrenia-like symptoms.

We found that excitatory neurotransmission onto DG GCs is subject to regulation by P2X7Rs at presynaptic sites, whereas P2X7R-mediated modulation is input specific. The potential regulatory mechanism involves the expression of P2X7 receptors in axon terminals and the modulation of influx of Ca^{2+} due to the direct activation of P2X7R by BzATP. In postnatal PCP injection-induced mice model of SCZ, we found that genetic ablation of P2X7Rs restored phencyclidine-induced perforant-GC synaptic alterations.

These findings pave the way for a better understanding of P2X7Rs in pathophysiology. The input-specific expression of neuronal P2X7Rs in the DG may indicate some specific functions of P2X7Rs in this region, providing a perspective for future studies. In addition, the modulatory effects of P2X7Rs on pathological conditions, such as SCZ-like disorders, provide potential therapeutic relevance.

6. Publications of the author

Publications related to the thesis

1. **Huang L**, Mut-Arbona P, Varga B, Torok B, Brunner J, Arszovszki A, Iring A, Kisfali M, Vizi ES, Sperlagh B. (2023) P2X7 purinergic receptor modulates dentate gyrus excitatory neurotransmission and alleviates schizophrenia-like symptoms in mouse. iScience, 26: 107560.11.2 (IF: 5.8)

2. Mut-Arbona P, **Huang L**, Baranyi M, Tod P, Iring A, Calzaferri F, de Los Rios C, Sperlagh B. (2023) Dual Role of the P2X7 Receptor in Dendritic OutgroWTh during Physiological and Pathological Brain Development. J Neurosci, 43: 1125-1142 (IF: 5.3)

3. Zhang Y, **Huang L**, Kozlov SA, Rubini P, Tang Y, Illes P. (2020) Acupuncture alleviates acid- and purine-induced pain in rodents. Br J Pharmacol, 177: 77-92. (IF: 8.740)